DOI: 10.1117/1.OE.57.3.037111

General multimode polarization splitter design in uniaxial media

Poliane A. Teixeira,[a,*] Daniely G. Silva,[a] Lucas H. Gabrielli,[b] Danilo H. Spadoti,[a] and Mateus A. F. C. Junqueira[a]
[a]Federal University of Itajubá, Institute of Systems Engineering and Information Technology, Itajubá, Minas Gerais, Brazil
[b]University of Campinas, School of Electrical and Computer Engineering, Campinas, São Paulo, Brazil

Abstract. Quasiconformal transformation optics is used to design two-dimensional polarization beam splitters. The resulting media present inhomogeneous uniaxial permittivity and nonmagnetic response. The compact devices are theoretically designed and investigated for symmetrical and asymmetrical geometries, with footprint of 64 and 110 μm^2, respectively. The polarization splitter performance is evaluated for the fundamental mode and third mode, exhibiting an insertion loss closer to 0 dB and extinction ratio above 40 dB over a broad wavelength range. [DOI: 10.1117/1.OE.57.3.037111]

Keywords: beam splitters; quasiconformal mapping; transformation optics; uniaxial medium.

Paper 171516 received Sep. 25, 2017; accepted for publication Mar. 6, 2018; published online Mar. 28, 2018.

1 Introduction

The polarization beam splitter (PBS) is a polarization-handling device that is able to split the incoming optical modes based on their polarization, i.e., transverse electric (TE) and transverse magnetic (TM) modes. This optical device is a key component largely used in optical communication systems. The polarization-division multiplexing technique[1] allows the use of polarization diversity for multiplexing channels, increasing the data transmission capacity in optical links and reducing the insertion losses.[2] The PBS also finds application in polarization sensitive devices, such as fiber-optic sensors,[3] quantum photonics integrated circuits,[4] and electro-optic detectors.[5]

However, the development of a compact PBS with low insertion loss and a high extinction ratio over a broad bandwidth is still a challenge. Different approaches to develop PBS have been reported, such as those that use the transformation optics (TO) technique,[6–9] directional coupler (DC),[10] multimode interference (MMI),[11,12] Mach–Zehnder interferometer (MZI),[13,14] gratings,[15,16] and tapered waveguide coupling.[17,18] A traditional DC has two straight waveguides with identical lengths preventing high extinction ratio. An alternative to enhance the extinction ratio is to use two or more cascaded stages,[10] but it makes the PBS longer and with a narrower bandwidth. Alternatively, the MMI-based PBS typically needs a phase shifter; therefore, the structure usually requires a high fabrication precision,[11] and it is large in the footprint area.[12] Another approach based on MZI also leads to large footprints,[13] even though, in some cases it can be implemented with relaxed tolerance.[14] The PBS designs based on waveguide gratings present lower coupling efficiency, a narrow wavelength range,[15] and it needs a high fabrication resolution,[16] similarly to PBSs developed from tapered waveguides.[17,18]

Apart from these cases, a PBS using a hybrid plasmonic Y-branch on a silicon-on-insulator (SOI) platform has been demonstrated.[19] The structure is formed by silicon and silver strip waveguides sandwiched with a silicon dioxide layer. It was found that the figures of merit of this device are dependent on the thicknesses of silicon dioxide layer and silver strip. Thus, the optimal values of insertion loss were below 2.35 dB and extinction rate of 10 dB in a bandwidth of 285 nm.

A different strategy proposed by Shen et al.[20] used the free-form metamaterials to experimentally obtain an ultracompact PBS with a footprint of 2.4×2.4 μm^2. The PBS is patterned on an SOI substrate, and it presents an extinction rate around 12 dB within a bandwidth of 32 nm.

Another concept used to create PBS is based on the application of photonic crystals.[21] In this approach, the polarization splitting is obtained with an operating bandwidth of 53 nm and maximum extinction rate of 23.64 dB. A dual-core photonic crystal fiber with holes filled with magnetic fluids was used to develop a tunable PBS,[22] and it was observed that the structure can reach an extinction rate >100 dB.

Zhang et al.[23] implemented a device that can work as a polarization splitter and rotator simultaneously, based on a silicon bent DC structure. The structure presents insertion loss lower than 0.3 dB in the wavelength of 1530 to 1600 nm. A PBS based on three cascaded bent DCs has also been demonstrated.[24] That device consists of SOI nanowires with a silicon dioxide upper cladding, and it has extinction rate values >20, 25, and 30 dB within the approximate bandwidths of 135, 95, and 70 nm, respectively. Beyond those, a PBS based on the DC uses the high birefringence property of lithium niobate ($LiNbO_3$) to separate the TE and TM polarizations.[25] The simulations showed that this device has an extinction rate >10 dB in a bandwidth of 65 nm. Additionally, a PBS based on an asymmetrical DC used silicon hybrid plasmonic waveguide and silicon nanowire.[26] An ultrasharp bend radius was added at the end of one port to improve the extinction ratio of the device. The PBS performance was evaluated through simulations, and an extinction

*Address all correspondence to: Poliane A. Teixeira, poliane_aires@yahoo.com.br

0091-3286/2018/$25.00 © 2018 SPIE

rate >12 dB and insertion loss <0.66 dB were obtained in a bandwidth of ∼120 nm.

Silicon-based slot waveguides are used to develop a PBS, and an asymmetric multimode waveguide is employed to separate the TE and TM modes.[27] In addition, tapered waveguide structures and S-bend are introduced into this PBS to achieve better performance. Numerical results showed that the device has a maximum extinction rate of 20.9 dB and insertion loss below 1.37 dB at the wavelength of 1550 nm.

Watanabe et al.[28] proposed an indium phosphide (InP)-based PBS using an MZI, which enables the easy individual adjustment of the TE polarization of the device. The used method allows positive and negative changes in the refractive index, due to the Pockels effects. A test sample was implemented and extinction rate of about 14 dB at the wavelength 1550 nm was exhibited. Another approach to realize a PBS using symmetric MZI on InP platform was presented.[29,30] For these projects, plasma dispersion effect and the Pockels effect in a p-i-n structure, whose bulk intrinsic region was inserted between the p-type and n-type layers, were used in order to do the polarization beam splitting. The experimental results showed an insertion loss of 3.5 dB and an extinction rate >15 dB over the entire C-band. In the same way, Pérez-Galacho et al.[31] implemented an asymmetrical MZI based on PBS, showing that thermal tuning can simultaneously compensate fabrication errors and achieve wavelength tunability. The experimental model presented extinction rate of 16 dB and insertion loss around 1.2 dB within C-band.

On the other hand, PBSs designed by TO are broadband with high extinction ratio and low insertion loss. With this technique, it is possible to choose the geometrical shape for each polarization, allowing great flexibility in the splitter design, which is useful to achieve compact devices. Nevertheless, designs with TO, in general, result in uncommon media requirements, which are not available in nature and cannot be easily fabricated even with metamaterials.[32]

TO is a technique used to design electromagnetic devices simply based on coordinate transformations, enabling the designer to control the propagation of waves.[33,34] One of the most investigated devices created from TO is the invisibility cloak.[32,33] Beyond the invisibility cloak, a great amount of devices have been realized via TO, such as perfect lenses,[35] waveguides,[36] compressors,[37] field rotators,[38] and collimators.[39] To allow such flexibility, TO designs generally require media with anisotropic permittivity and permeability. Nevertheless, such media can be avoided with the quasiconformal transformation optics (QCTO) technique,[40] which reduces the anisotropy of the media and allows it to be described by a graded refractive index.

Kwon and Werner[6] used a nonconformal coordinate transformation to realize a PBS via TO but obtained a medium with anisotropic magnetic response, representing a challenge to be implemented in practice. Another PBS design based on TO was proposed by Zhou et al.,[7] where the medium presents inhomogeneous anisotropic permeability and vacuum permittivity. Furthermore, some terms in the permeability tensor have negative values, also rendering it impractical to be manufactured. The PBS proposed by Wu et al.[8] makes use of a linear coordinate transformation to design a homogeneous anisotropic medium. Its properties for the TE polarization are the same as vacuum, but for the TM polarization, a homogeneous anisotropic material is necessary. A drawback of this approach is that again a few off-diagonal terms in the permittivity tensor have negative values, leading to uncommon media requirements, not available in nature. Moreover, reflections are still observed at the output boundary of the device. Recently, Eskandari et al.[9] designed a PBS with a nonmagnetic, homogeneous, and reflectionless medium with reduced anisotropy. However, once again, the off-diagonal terms ε_{xy} and ε_{yx} also present negative values.

For integrated photonics, there are numerous PBS manufactured in the SOI platform, due to the advantages of being compatible with the complementary metal–oxide–semiconductor fabrication process and offering a compact footprint, owing to the high index contrast between Si and SiO_2.[12,13,17] However, other materials can also be used in PBS implementation, such as $LiNbO_3$[25,41] and III–V semiconductor compounds,[42] which is desirable to enable low-cost photonic integrated circuits. Another design possibility for obtaining a PBS is based on effective medium theory,[43,44] on which the effective refractive index values for the TE and TM polarizations may be different and calculated by effective medium theory.[45]

In this paper, two-dimensional (2-D) QCTO is used to design the PBS. This approach eliminates the magnetic response, and the permittivity tensor becomes uniaxial facilitating the device manufacture. Due the application of QCTO, one can consider that the proposed device can operate at any wavelength.[40] The use of TO to create the PBS guarantees an insertion loss closer 0 dB, an extinction ratio above 40 dB, and it preserves the propagation mode characteristics over a wide wavelength range. Two examples of compact PBS, one symmetric and one asymmetric, with footprints of 64 and 110 μm^2, respectively, are presented. The device performances are analyzed under the fundamental mode and third mode for each polarization.

2 Theoretical Basis

From the TO theory, the medium properties after a coordinate transformation are[33]

$$\varepsilon' = \frac{J^T \varepsilon J}{\det(J)}, \qquad \mu' = \frac{J^T \mu J}{\det(J)}, \tag{1}$$

where J is the Jacobian matrix of the coordinate transformation, which represents the wave propagation, and ε and μ are the original medium parameters.

If the coordinate transformation is nonconformal, the material properties defined in Eq. (1) are anisotropic. However, if a quasiconformal mapping is used, the medium can become quasi-isotropic and it can be implemented using dielectric materials.

The design principle of PBS starts from the fact that Maxwell's equations can be separated in two polarizations for 2-D geometries. Considering the work plane as the xy plane, the TE mode is affected by material parameters ε_{zz}, μ_{xx}, μ_{xy}, μ_{yx}, and μ_{yy}, and the TM mode interacts with the material parameters μ_{zz}, ε_{xx}, ε_{xy}, ε_{yx}, and ε_{yy}.[6] As each polarization is affected by disjoints sets of parameters, they can be separately controlled. The PBS explores this situation by being defined as a superposition of two waveguides one for each polarization, with identical inputs and separate outputs. The corresponding properties for each

arm are defined by TO using one coordinate transformation for each polarization. If a quasiconformal mapping is used, the TE mode is affected only by $\epsilon_{zz} = n_{zz}^2$ and the TM mode is affected only by $\epsilon_{xx} = \epsilon_{yy} = n_{xx}^2 = n_{yy}^2$. In this case, these properties are evaluated as

$$\varepsilon'_{zz} = \varepsilon\left[\left(\frac{\partial x'_e}{\partial x}\right)^2 + \left(\frac{\partial x'_e}{\partial y}\right)^2\right]^{-1},$$
$$\varepsilon'_{xx} = \varepsilon'_{yy} = \varepsilon\left[\left(\frac{\partial x'_m}{\partial x}\right)^2 + \left(\frac{\partial x'_m}{\partial y}\right)^2\right]^{-1}, \quad (2)$$

where the subscript e and m indicate the coordinates transformation for the TE and TM modes, respectively. The proposed design reduces anisotropy for each polarization, but the final device will necessarily have $\varepsilon_{xx} = \varepsilon_{yy} \neq \varepsilon_{zz}$. Nonetheless, the off-diagonal terms in the permittivity matrix vanish, and therefore, the resulting medium is uniaxial.

In this work, the QCTO is applied, and the original medium is considered a dielectric slab waveguide as shown in Fig. 1, where the thickness in the z-axis is, in principle, assumed as infinite. The wave propagation occurs in the y-axis.

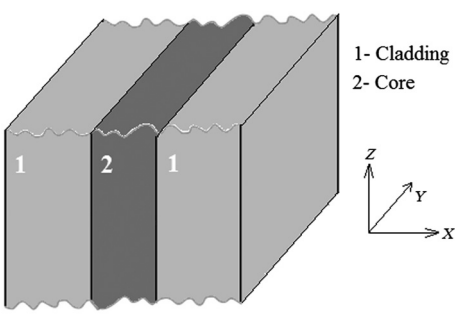

Fig. 1 Overview of the original medium as a dielectric slab waveguide.

With QCTO application, it is possible to design a symmetrical PBS, in which one waveguide shifts the TE mode to the left and another shifts the TM mode to the right, according to Fig. 2(a). It is also possible to design an asymmetrical PBS, as shown in Fig. 2(b); in such case, a waveguide for the TE mode shifts to the left and expands the mode while another waveguide for the TM mode is bent to the right. Figure 2 consists in a 2-D view of the obtained device, which should be assumed as infinite in the z-direction.

Using the technique demonstrated by Junqueira et al.[46] to design waveguides, the initial coordinate transformations for the symmetrical PBS are defined (in μm) as

$$(f_{x_e}; f_{y_e}) = \left[(2+x)\left(\frac{y}{10}\right) + x\left(1 - \frac{y}{10}\right); y\right],$$
$$(f_{x_m}; f_{y_m}) = \left[(-2+x)\left(\frac{y}{10}\right) + x\left(1 - \frac{y}{10}\right); y\right], \quad (3)$$

where the output at $y = 10$ μm is shifted by 2 μm to the left for the TE mode and 2 μm to the right for the TM mode. For the 2-D asymmetrical PBS, the initial transformations for the TE and TM modes are (in μm)

$$(f_{x_e}; f_{y_e}) = \left[\left(-2 + \frac{3}{2}x\right)\frac{y}{10} + x\left(1 - \frac{y}{10}\right); y\right],$$
$$(f_{x_m}; f_{y_m}) = \left[\frac{7y}{10} + x\left(1 - \frac{y}{10}\right); (7-x)\frac{y}{10}\right], \quad (4)$$

where the TE mode is again shifted 2 μm to the left and introduces a beam waist broadening of 50%, whereas the TM waveguide undergoes a 90-deg bend to the right.

The initial transformations in Eqs. (3) and (4) are nonconformal, resulting in anisotropic permittivity and permeability. Nevertheless, they have the boundary conditions necessary to describe the device functionality with reflectionless interfaces. Applying an anisotropy minimization technique,[46] the

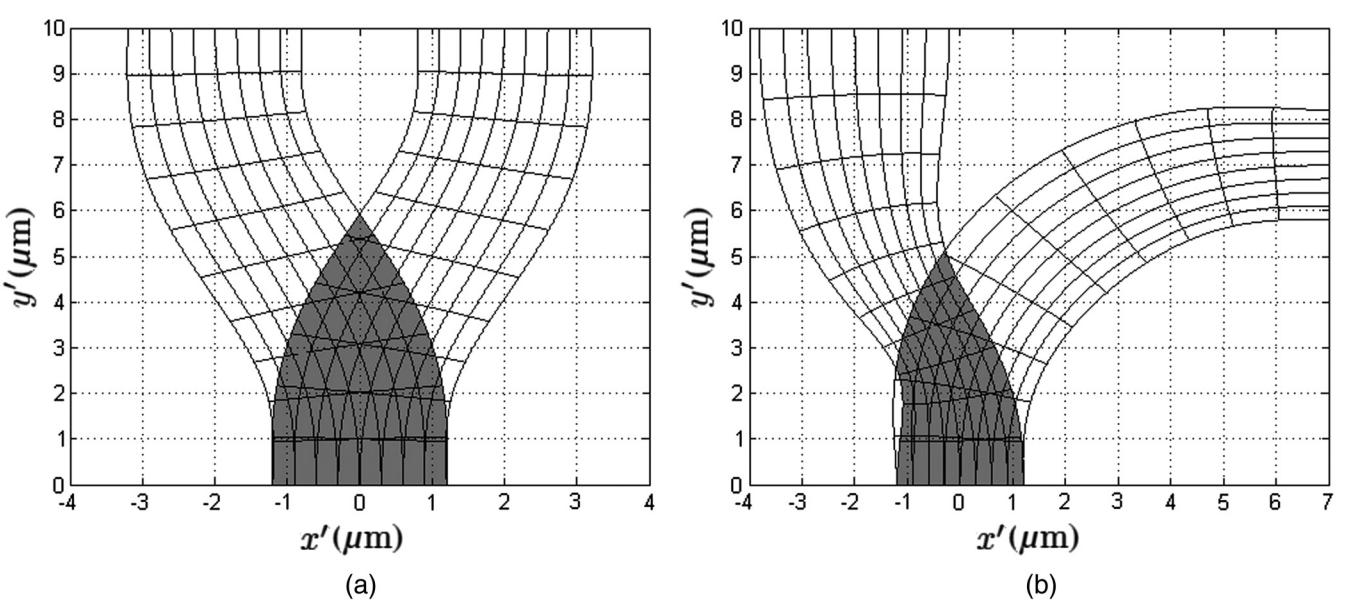

Fig. 2 Quasiconformal coordinate transformation for each polarization, highlighting the anisotropic index region: (a) symmetrical and (b) asymmetrical PBS designs.

optimized coordinate transformation x'_e and y'_e for the TE mode and x'_m and y'_m for the TM mode can be used in Eq. (2) to define the PBS as a uniaxial medium, which occurs only in the region where both waveguides intersect, as shown by the highlighted regions (gray) in Fig. 2. All remaining areas can be implemented from isotropic materials, because they support only one of the polarizations. For the uniaxial region, one could consider the use of naturally occurring uniaxial materials, such as $LiNbO_3$,[41] or layered metamaterials for manufacturing.

3 Numerical Results

The PBSs were obtained after QCTO application over a dielectric slab waveguide with an 800-nm-wide core with refractive index of 2.5. The cladding for the original slabs of the symmetrical and asymmetrical PBSs had indices of 1.5 and 1.7, respectively.

After the transformation, the refractive index map for each PBS example is presented in Fig. 3 for both the TE ($n_{zz} = \sqrt{\varepsilon_{zz}}$) and TM ($n_{xx} = \sqrt{\varepsilon_{xx}}$) modes. The symmetrical PBS [Figs. 3(a) and 3(b)] ends up requiring a graded refractive index raging between 2.57 and 1.30. The asymmetrical PBS index ranges from 1.08 to 3.28. These values of minimal and maximal refractive indices can be found in an SOI platform. Furthermore, as mentioned earlier, the proposed medium has uniaxial properties and may be implemented from appropriate materials with effective medium theory.

The PBS examples were simulated using the finite-element method for a wavelength $\lambda = 1550$ nm. The normalized electromagnetic field distributions for each polarization in the fundamental modes are shown in Fig. 4. In Fig. 4(a), the TE mode is shifted by 2 μm to the left is presented, and in Fig. 4(b), the TM mode is shifted by 2 μm to the right in the symmetrical PBS design. For the asymmetrical PBS, the output for TE mode is shifted by 2 μm to the left, and the output for TM mode undergoes a 90-deg bend to the right.

Because the TO technique does not depend on wavelength or propagation constants, the devices, thus, designed should be inherently wavelength and mode independent (except for material dispersion effects). To verify that the presented PBSs work for higher-order modes, the results for the excitation of the third-order mode of the slabs are presented in Fig. 5. We note that each mode is guided according to its polarization in the exact same fashion as for the fundamental modes. Due to the weaker confinement of those modes, we can see that their respective insertion losses will not be optimal but that is a limitation of the original slab waveguide, which operates close to cutoff for the third-order modes, and not the PBS designs.

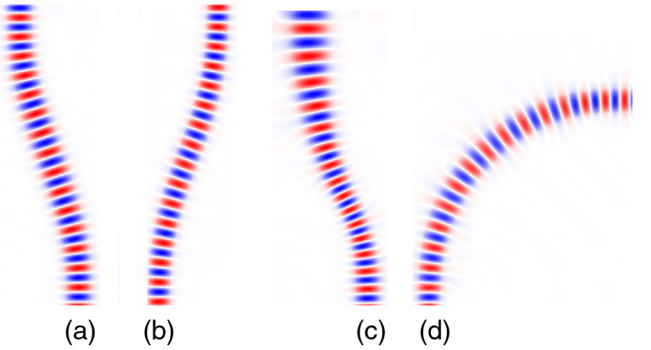

Fig. 4 Normalized electromagnetic field distributions for PBS analyzed on the fundamental mode. Symmetrical PBS: (a) out-of-plane component of the electric field (TE mode) and (b) out-of-plane component of the magnetic field (TM mode). Asymmetrical PBS: (c) out-of-plane component of the electric field (TE mode) and (d) out-of-plane component of the magnetic field (TM mode).

The total power flow is also demonstrated through the Poynting vector magnitude plotted in Fig. 6 for both geometries, polarizations, and mode orders as before. In these examples, the TE and TM modes are excited simultaneously and with equal powers; therefore, each arm should carry half of the incident power. The deviations from the ideal responses are results of the residual anisotropy, and for the high-order modes, the extensive evanescent tails of each mode leaving the transformed region.

To quantify the performance of the devices, Table 1 presents the insertion losses for each one of the modes studied in the proposed geometries with $\lambda = 1460$ nm, $\lambda = 1550$ nm, and $\lambda = 1625$ nm, respectively.

Table 1 shows insertion losses close to zero for all studied cases. They were not exactly zero due to residual anisotropy

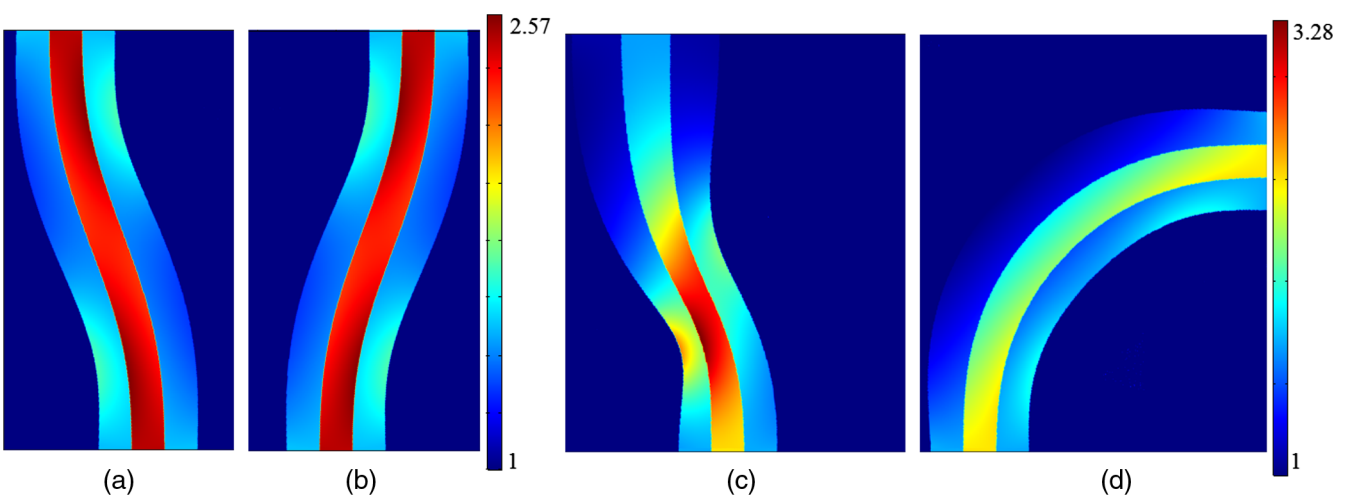

Fig. 3 Components of the refractive index tensor. Symmetrical PBS: (a) n_{zz} and (b) $n_{xx} = n_{yy}$. Asymmetrical PBS: (c) n_{zz} and (d) $n_{xx} = n_{yy}$.

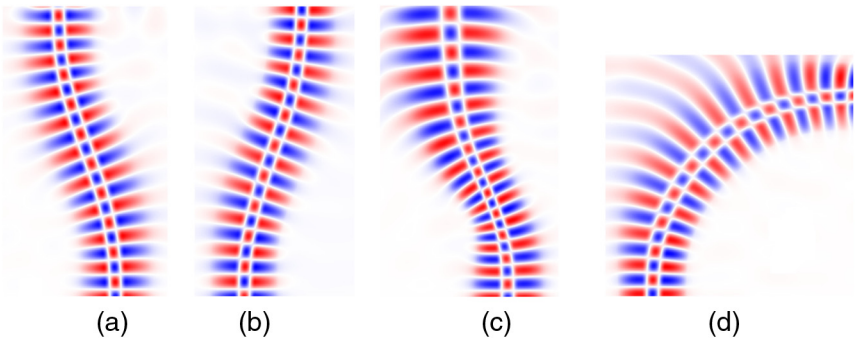

Fig. 5 Same as in Fig. 4 but for the third-order mode for each polarization.

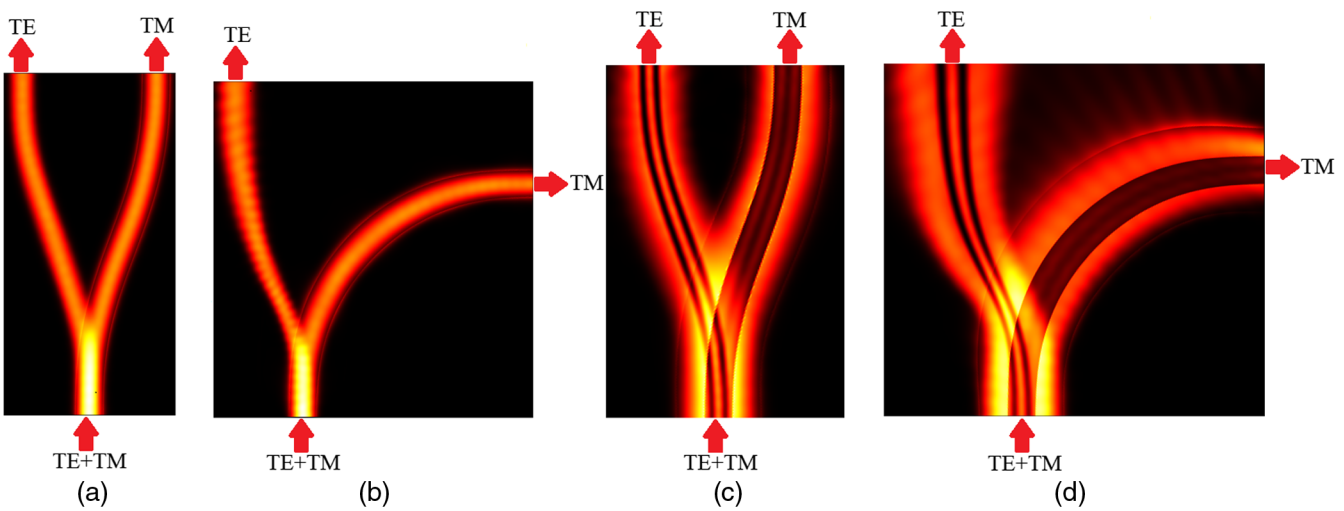

Fig. 6 Poynting vector normalized magnitude distribution: (a) symmetrical PBS with fundamental mode, (b) asymmetrical PBS with fundamental mode, (c) symmetrical PBS with third mode, and (d) asymmetrical PBS with third modes.

Table 1 Insertion losses for all supported modes in both devices for different wavelengths.

	Symmetrical PBS (dB)			Asymmetrical PBS (dB)		
Mode	1460 nm	1550 nm	1625 nm	1460 nm	1550 nm	1625 nm
TE_1	0.03	0.04	0.06	0.07	0.03	0.13
TE_3	0.05	0.06	0.09	0.17	0.19	0.22
TM_1	0.03	0.04	0.06	0.08	0.02	0.14
TM_3	0.05	0.06	0.09	0.16	0.18	0.20

resulting from quasiconformal mapping, which induces some scattering of the fields. Moreover, the extinction ratio was above 40 dB for all cases, and its values were also affected by the residual anisotropy.

To evaluate the PBS performance in a more realistic three-dimensional geometry, the behavior of the extinction ratio in relation to the increase of the waveguide thickness was analyzed. The results show a convergence to 40 dB for the extinction rate when the thickness increases. This is an expected result, since it approximated for the values found in the 2-D simulations, in which the thickness is considered infinite. This analysis was done in the asymmetric PBS at $\lambda = 1625$ nm for the fundamental mode and third mode as shown in Fig. 7. Furthermore, the insertion loss was practically unaffected by the thickness modification, since this loss, in the simulations, is attributed to the inherent residual anisotropy of the quasiconformal mapping.

Finally, a comparison is given in Table 2 for different structures used to create PBS, summarizing some reported results of the PBSs and comparing them with our work. In this paper, we show a splitter which simultaneously presents: low insertion loss, high extinction rate, broadband and multimode. All these properties together represent an important improvement with respect to those found in the literature.

4 Conclusion

The QCTO enables the design of PBS without magnetic response and with uniaxial refractive index. The ability of choosing arbitrary shape for each polarization TE and TM ensures flexibility in the design, allowing compact and small footprint devices. The designed PBS has insertion loss closer to 0 dB and extinction ratio above 40 dB in a broad bandwidth, since it was designed with TO, which makes its application attractive in optical communication systems.

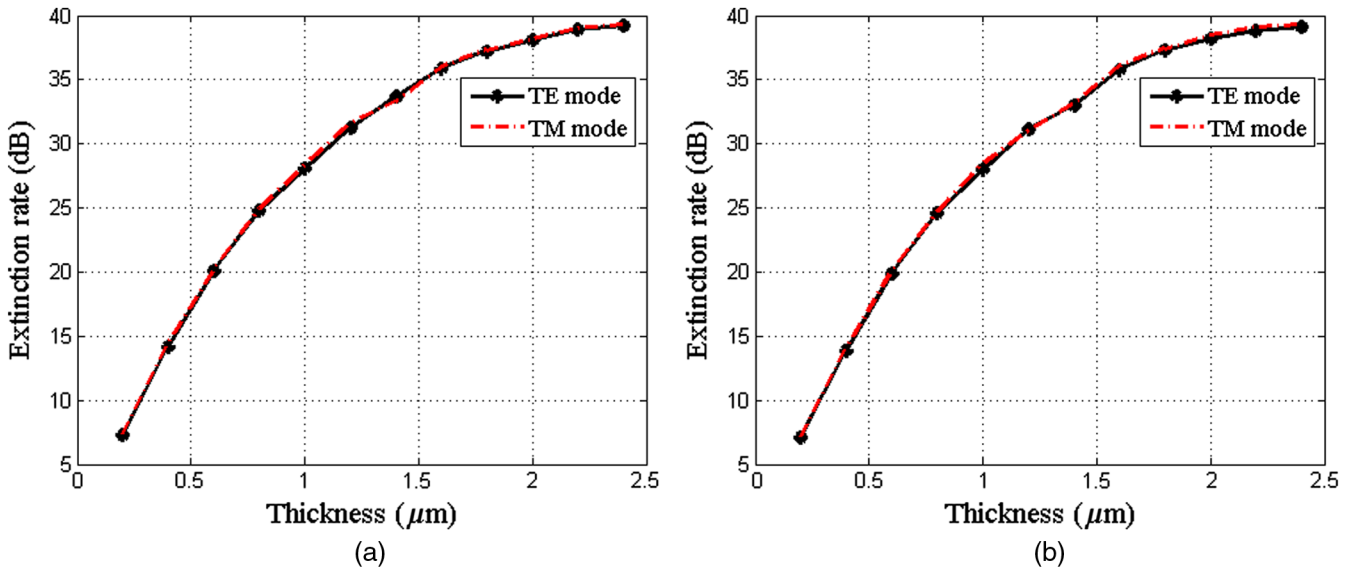

Fig. 7 Extinction rate as a function of the thickness variation for $\lambda = 1625$ nm. (a) Asymmetrical PBS with fundamental mode and (b) asymmetrical PBS with third mode.

Table 2 Comparison of some PBS structures.

Structure	Insertion loss (dB)	Extinction ratio (dB)	Bandwidth (nm)	Multimode	Experimental demonstration
Hybrid plasmonic Y-branch[19]	<2.35	10	285	No	No
Free-form metamaterials[20]	N/A	~12	32	No	Yes
Photonic crystals[21]	N/A	≤23.64	53	No	No
Dual-core photonic crystal fiber[22]	N/A	>100	N/A	No	No
Bent DC[23]	<0.3	N/A	70	No	Yes
Three cascaded bent DCs[24]	N/A	>20	~135	No	Yes
		>25	~95		
		>30	~70		
DC[25]	N/A	>10	65	No	No
Asymmetrical DC[26]	<0.66	>12	~120	No	No
Asymmetric multimode waveguide[27]	<1.37	≤20.9	C-Band	Yes	No
MZI[28]	N/A	~14	N/A	No	Yes
Symmetric MZI[29,30]	3.5	>15	C-Band	No	Yes
Asymmetric MZI[31]	~1.2	16	C-Band	No	Yes
This work	<0.22	>40	C-Band	Yes	No

Furthermore, the designed PBS can support higher-order modes, allowing applications in mode-division multiplexing.

Acknowledgments

The authors thank the National Council of Technological and Scientific Development (CNPq), the Coordination for the Improvement of Higher Education Personnel (CAPES), and the Foundation for Research Support of Minas Gerais (FAPEMIG) for their financial support.

References

1. D. Sim, H. Kim, and Y. Chung, "Direct-detection receiver for polarization-division-multiplexed OOK signals," *IEEE Photonics Technol. Lett.* **27**, 2238–2241 (2015).
2. M.-S. Lai and C.-C. Huang, "Submicron-scale broadband polarization beam splitter using CMOS-compatible materials," *Sci. Rep.* **7**, 4531 (2017).
3. C. Li et al., "Error analysis and experiment for reflective Sagnac interferometer-type fiberoptic current sensor," in *Int. Conf. on Electronics and Optoelectronics (ICEOE '11)*, Vol. 2, IEEE (2011).
4. L.-T. Feng et al., "On-chip coherent conversion of photonic quantum entanglement between different degrees of freedom," *Nat. Commun.* **7**, 11985 (2016).

5. J. Mabon and R. A. Lewis, "Effect of non-ideal beamsplitters in THz electro-optic detectors," in *40th Int. Conf. on Infrared, Millimeter, and Terahertz Waves (IRMMW-THz '15)*, pp. 1–2, IEEE (2015).
6. D. H. Kwon and D. H. Werner, "Polarization splitter and polarization rotator designs based on transformation optics," *Opt. Express* **16**, 18731–18738 (2008).
7. J. Zhou et al., "Design of a new kind of polarization splitter based on transformation optics," *Optik–Int. J. Light Electron Opt.* **122**, 1672–1675 (2011).
8. Y. Wu et al., "Controlling the wave propagation through the medium designed by linear coordinate transformation," *Eur. J. Phys.* **36**, 015006 (2015).
9. H. Eskandari, M. S. Majedi, and A. R. Attari, "Design of reflectionless non-magnetic homogeneous polarization splitters with minimum anisotropy based on transformation electromagnetics," *J. Opt. Soc. Am. B* **34**, 1191–1198 (2017).
10. H. Wu and D. Dai, "Novel high-performance polarization beam splitter on silicon," in *Asia Communications and Photonics Conf. 2016*, Optical Society of America (2016).
11. Y. Ding, H. Ou, and C. Peucheret, "Wideband polarization splitter and rotator with large fabrication tolerance and simple fabrication process," *Opt. Lett.* **38**, 1227–1229 (2013).
12. W. Yang et al., "A compact and wide-band polarization beam splitter based on wedge-shaped MMI coupler in silicon-on-insulator," in *Optical Fiber Communication Conf.*, Optical Society of America (2015).
13. D. Dai et al., "Compact polarization beam splitter using an asymmetrical Mach–Zehnder interferometer based on silicon-on-insulator waveguides," *IEEE Photonics Technol. Lett.* **24**, 673–675 (2012).
14. D. Pérez-Galacho et al., "Integrated polarization beam splitter with relaxed fabrication tolerances," *Opt. Express* **21**, 14146–14151 (2013).
15. D. Taillaert et al., "A compact two-dimensional grating coupler used as a polarization splitter," *IEEE Photonics Technol. Lett.* **15**, 1249–1251 (2003).
16. Y. Zhang et al., "High-extinction-ratio silicon polarization beam splitter with tolerance to waveguide width and coupling length variations," *Opt. Express* **24**, 6586–6593 (2016).
17. W. D. Sacher et al., "Polarization rotator-splitters in standard active silicon photonics platforms," *Opt. Express* **22**, 3777–3786 (2014).
18. C. Sun et al., "A low crosstalk and broadband polarization rotator and splitter based on adiabatic couplers," *IEEE Photonics Technol. Lett.* **28**, 2253–2256 (2016).
19. T. Hu et al., "A compact ultrabroadband polarization beam splitter utilizing a hybrid plasmonic y-branch," *IEEE Photon. J.* **8**, 1–9 (2016).
20. B. Shen et al., "An integrated-nanophotonics polarization beamsplitter with $2.4 \times 2.4\ \mu m^2$ footprint," *Nat. Photonics* **9**, 378–382 (2015).
21. U. G. Yasa et al., "High extinction ratio polarization beam splitter design by low-symmetric photonic crystals," *J. Lightwave Technol.* **35**, 1677–1683 (2017).
22. J. Wang et al., "A tunable polarization beam splitter based on magnetic fluids-filled dual-core photonic crystal fiber," *IEEE Photon. J.* **9**, 1–10 (2017).
23. Y. Zhang et al., "Ultra-compact and highly efficient silicon polarization splitter and rotator," *APL Photonics* **1**, 091304 (2016).
24. H. Wu, Y. Tan, and D. Dai, "Ultra-broadband high-performance polarizing beam splitter on silicon," *Opt. Express* **25**, 6069–6075 (2017).
25. Z. Gong et al., "Optimal design of DC-based polarization beam splitter in lithium niobate on insulator," *Opt. Commun.* **396**, 23–27 (2017).
26. X. Guan et al., "Ultracompact and broadband polarization beam splitter utilizing the evanescent coupling between a hybrid plasmonic waveguide and a silicon nanowire," *Opt. Lett.* **38**, 3005–3008 (2013).
27. Y. Xu, J. Xiao, and X. Sun, "Compact polarization beam splitter for silicon-based slot waveguides using an asymmetrical multimode waveguide," *J. Lightwave Technol.* **32**, 4884–4890 (2014).
28. K. Watanabe et al., "Easy adjustment structure and method for realizing InP based polarization beam splitter via Pockels effect dependence on crystal orientation," *Jpn. J. Appl. Phys.* **55**, 08RB04 (2016).
29. N. Abadía et al., "Highly fabrication tolerant InP based polarization beam splitter based on p-i-n structure," *Opt. Express* **25**, 10070–10077 (2017).
30. N. Abadía et al., "Novel polarization beam splitter based on p-i-n structure for an indium phosphide platform," in *19th Int. Conf. on Transparent Optical Networks (ICTON '17)*, pp. 1–4 (2017).
31. D. Pérez-Galacho et al., "Integrated polarization beam splitter for 100/400 GE polarization multiplexed coherent optical communications," *J. Lightwave Technol.* **32**, 361–368 (2014).
32. D. Schurig et al., "Metamaterial electromagnetic cloak at microwave frequencies," *Science* **314**, 977–980 (2006).
33. U. Leonhardt and T. Philbin, *Geometry and Light: The Science of Invisibility*, Dover Publications, New York (2010).
34. J. B. Pendry, D. Schurig, and D. R. Smith, "Controlling electromagnetic fields," *Science* **312**, 1780–1782 (2006).
35. J. Hunt, G. Jang, and D. R. Smith, "Perfect relay lens at microwave frequencies based on flattening a Maxwell lens," *J. Opt. Soc. Am. B* **28**, 2025–2029 (2011).
36. M. Junqueira, L. Gabrielli, and D. Spadoti, "Comparison of anisotropy reduction strategies for transformation optics designs," *IEEE Photonics J.* **7**, 1–10 (2015).
37. D. Liu et al., "Transformation inverse design," *Opt. Express* **21**, 14223–14243 (2013).
38. H. Chen and C. Chan, "Transformation media that rotate electromagnetic fields," *Appl. Phys. Lett.* **90**, 241105 (2007).
39. D.-H. Kwon and D. H. Werner, "Transformation optical designs for wave collimators, flat lenses and right-angle bends," *New J. Phys.* **10**, 115023 (2008).
40. J. Li and J. B. Pendry, "Hiding under the carpet: a new strategy for cloaking," *Phys. Rev. Lett.* **101**, 203901 (2008).
41. Z. Gong et al., "Polarization beam splitter based on lithium niobate thin film," in *15th Int. Conf. on Optical Communications and Networks (ICOCN)*, pp. 1–3 (2016).
42. F. Ghirardi et al., "Polarization splitter based on modal birefringence in InP/InGaAsP optical waveguides," *IEEE Photonics Technol. Lett.* **5**, 1047–1049 (1993).
43. S. M. Rytov, "Electromagnetic properties of a finely stratified medium," *J. Exp. Theor. Phys.* **2**, 466–475 (1956).
44. X. Zhang and Y. Wu, "Effective medium theory for anisotropic metamaterials," *Sci. Rep.* **5**, 7892 (2015).
45. Z. Hua-Jun et al., "Optimal design of sub-wavelength metal rectangular gratings for polarizing beam splitter based on effective medium theory," *Chin. Phys. B* **18**, 5326–5330 (2009).
46. M. A. F. C. Junqueira, L. H. Gabrielli, and D. H. Spadoti, "Anisotropy minimization via least squares method for transformation optics," *Opt. Express* **22**, 18490–18498 (2014).

Poliane A. Teixeira received her BSc and MSc degrees in electrical engineering from Inatel, Brazil, in 2010 and 2015, respectively. She is a doctorand of electrical engineering at Unifei, Brazil. In 2011, she joined the Nitere Ltd. as a research and development engineer on a touch-screen project. From 2015 to 2017, she was a professor at Faculdade de Extrema. Since 2016, she has been working on the polarization splitter designs through quasiconformal transformation optics.

Daniely G. Silva received her BSc and MSc degrees in electrical engineering from Inatel, Brazil, in 2007 and 2013, respectively. She is a doctorand of electrical engineering at Unifei, Brazil. In 2007, she joined the Inatel as a research and development engineer on digital communication and mixed signal IC projects. Since 2016, she has been working on the 3-D invisibility cloak design with numerical optimization. Her areas of interest include optical devices, nanophotonics, and communication systems.

Lucas H. Gabrielli is a professor at the School of Electrical and Computer Engineering in UNICAMP since 2013. He graduated magna cum laude in electronics engineering from ITA in 2006, received his master's degree from UNICAMP in 2008 and Cornell University in 2012, and his PhD from Cornell University in 2012. He has been an associate director of the Center for Semiconductor Components and Nanotechnologies since 2016. His research focus is nanophotonics for communications and sensing.

Danilo H. Spadoti graduated in electrical engineering at UNIFEI in 2002, received his master's degree in 2004, and his PhD in 2008 in electrical engineering at USP. In 2009, he did his postdoctoral in Nanophotonics Groups at Cornell University, USA. In 2010, he obtained a postdoctoral scholarship at Mackenzie University. Currently, he is an associate professor in the area of telecommunications systems and applied electromagnetics at UNIFEI. He has experience in electrical engineering and optical telecommunications, mainly in the following areas: optical communications, photonics, fiber optics, and silicon photonics.

Mateus A. F. C. Junqueira graduated in industrial engineering in 2009, computer engineering in 2011, and electrical engineering in 2013 from UNIFEI, received his master's degree in computer science from UNIFEI in 2012, and his PhD in electrical engineering from UNIFEI in 2015. Currently, he is an adjunct professor in the area of telecommunications systems at UNIFEI. He has been working in electrical engineering, mainly in the following areas: nanophotonics, distributed computing, telecommunications systems, numeric optimization, and electromagnetism.